FUDMA Journal of Sciences (FJS)
ISSN online: 2616-1370
ISSN print: 2645 - 2944
Vol. 10 No. 5, March, 2026, pp 353 – 365
DOI: https://doi.org/10.33003/fjs-2026-1005-5018

INVESTIGATION OF THE LATERAL EXTENT OF A COAL SEAM USING ELECTRICAL RESISTIVITY IMAGING AT MOLKO VILLAGE, GONGOLA BASIN NORTH EASTERN NIGERIA.

***[1]Buhari Garba, [2]Aminu L Ahmed and [3]Raimi Jimoh**

National Space Research and Development Agency, Obasanjo Space Centre, Pyakasa Junction Airport Road, Abuja P.M.B 437, Garki, Abuja.
Zonal Advanced Space Technology and Application kashere Gombe State.
Department of physics, Ahmadu Bello University Zaria.

* Corresponding Author email: buharigarba205@gmail.com

ABSTRACT

Subsurface uncertainty in the Gombe Formation, particularly within the Gongola Sub-basin of the Upper Benue Trough, presents significant challenges for coal exploration due to the formation's complex and heterogeneous nature. The Gombe Formation consists of a rapidly changing sequence of sandstones, shales, mudstones, and coal seams. Two-dimensional (2D) electrical resistivity imaging was conducted to detect and delineate the lateral extent of the coal seam, utilizing a dipole-dipole array. This protocol was chosen because of its high sensitivity to resistivity variations beneath the electrodes in each dipole pair. The ABEM Terrameter SAS 4000 was used for data acquisition, while Res2Dinv software was employed for data processing. Additionally, a borehole (BH) was used in this study to integrate the results and produce a clearer interpretation. Measurements were successfully conducted across five profiles using 21 electrodes. Profile one covered a distance of 525 m; profile two, 315 m; profile three, 420 m; profile four, 315 m; and profile five, 315 m, with an inter-electrode spacing of 5 m. The 2D electrical resistivity pseudosection model revealed resistivity values associated with coal ranging from 400 Ω·m to 1000 Ω·m at depths of approximately 20 m to 25 m, with an average thickness of 2 m to 4 m. The coal seam extends laterally over a distance of 252 m, with the deposit being more prominent in the eastern part of the study area. The resistivity variations observed in this study align well with findings from previous research on coal resistivity.

Keywords: Oral Gombe Formation, Electrical Resistivity, Lateral Extent, Coal Seam

INTRODUCTION

Coal is formed from decomposed plants and trees buried beneath the Earth's surface millions of years ago, making it an organic sedimentary rock (Hatcher and Clifford, 1997). The extraction of coal is a non-renewable process, and burning coal significantly contributes to climate change by emitting carbon dioxide, a potent greenhouse gas that plays a critical role in global warming. However, coal remains a valuable global energy resource for alleviating energy poverty in developing countries. Economic empowerment through access to energy is essential to ending energy poverty while simultaneously reducing emissions to address climate change. Developed countries rely less on fossil fuels for power generation, whereas emerging economies should aim to limit the production and consumption of fossil fuels. In India, coal accounts for 55% of the country's energy needs, making coal production vital for economic growth and development (Miller, 2005). Globally, coal contributes to over one-third of electricity generation (Aberšek and Flogie, 2022).

Geologically, coal occurs in strata and exhibits significantly different petrophysical properties compared to the surrounding rocks typically found in sedimentary basins (Hatherly, 2013). Its exploration requires advanced prospecting techniques to obtain the necessary data. Various methods—including geological, geochemical, geophysical, and drilling techniques—are employed to evaluate coal deposits. Notably, the electrical properties of coal have been identified as important for accurate characterization during mining operations (Tiwary, 1993). Geophysical techniques are particularly valuable in environmental studies and conventional geotechnical testing because they use non-invasive, cost-effective methods to investigate the subsurface (Anderson et al., 2008; Arjwech et al., 2013; Arjwech & Everett, 2015).

In coal investigations, it is advantageous to conduct studies before coal mining begins (Lei, 2015). Mohammed et al., (2016) al. electrical employed the method utilizing method, utilizing the the protocol, the strike direction of coal of coal in a part over Tai of Nigeria subsurface Nigeria. Subsurface the Gombe formation from Formation arises tectonic structural deformation high deformation, lithological variations (alternating sands, shales, and coal and coal), limited availability of high quality high-quality These factors make it difficult to map to accurately lateral The discovery of proven coal reserve and reserves exploration activities at the in basin uncover Basin have uncovered gaps in the stratigraphy of the Gombe Formation. Therefore, there is a need to further understand lateral understand the and distributions of distribution coals coal sediments sandy-shaly the study area from Gombe within formation from Formation. The discovery of proven coal reserves and recent exploration activities in the Gongola Basin have addressed some gaps in the stratigraphy of the Gombe Formation. Therefore, there is a need to further understand the lateral variations and distribution of coal and sandy-shaly sediments within the study area of the Gombe Formation. Estimating the volume of economically extractable coal remains a challenging task. Consequently, it is essential to delineate the coal seam in the subsurface to determine the direction of coal extension. Delineating the coal seam can also reveal any coal splitting and provide information about the seam's dip.

Coal splitting occurs when a coal seam is divided into two or more seams by a non-coal layer. This phenomenon results from interruptions in clastic sedimentation during organic accumulation, which may happen once or multiple times during the deposition of the coal seam (Thomas, 2012). Geo-electrical resistivity surveys are widely used in mineral exploration and have also been applied in geohydrology,

environmental science, and engineering (Adli et al., 2010). The resistivity survey method measures the potential difference created by electric currents passing through the subsurface. Current is injected into the ground through two current electrodes, and the potential difference between two other electrodes is recorded. From these measurements, the resistivity between two points can be calculated. The resistance at a specific subsurface location is determined from the measured voltage (V) and current (I) values.

In this research, the geophysical method employed is Electrical Resistivity. The high resistivity values of coal seams, compared to the surrounding sedimentary rock strata, make them highly responsive to electrical resistivity surveys. This responsiveness allows the coal seams to be easily detected in the results and clearly differentiated from other rock types. The main objective of this study is to detect and delineate the lateral extent, depth, and thickness of coal seams in the Gongola Basin within the Gombe Formation. Figure 1 illustrates how the science of geophysics applies the principles of physics to the study of the Earth. Geophysical investigations of the Earth's interior involve taking measurements at or near the Earth's surface that are influenced by the internal distribution of physical properties. Analysis of these measurements can reveal how the physical properties of the Earth's interior vary both vertically and laterally (Kearey et al., 2002). Exploration geophysics is the practical application of physical methods such as seismic, gravitational, magnetic, electrical, and electromagnetic techniques to measure the physical properties of rocks, particularly to detect measurable physical differences between rocks that contain ore deposits or hydrocarbons and those that do not.

The purpose of electrical resistivity surveys is to determine the subsurface resistivity distribution by making measurements on the ground surface (Figure 2). From these measurements, the true resistivity of the subsurface can be estimated. Ground resistivity is influenced by various geological parameters, such as mineral and fluid content, porosity, and the degree of water saturation in the rock (Loke and Barker, 1996). The resistivity method involves measuring the potential difference between one pair of electrodes while transmitting direct current (DC) between another pair. In homogeneous ground, the depth of penetration is proportional to the separation between the electrodes, and varying the electrode spacing provides information about the stratification of the subsurface. The measured quantity is called apparent resistivity. Interpreting resistivity data involves two steps: a physical interpretation of the measured data, resulting in a physical model, and a geological interpretation of the derived physical parameters (Dahlin, 2001). Electrical resistivity surveys are generally conducted using two methods: resistivity profiling and resistivity depth sounding.

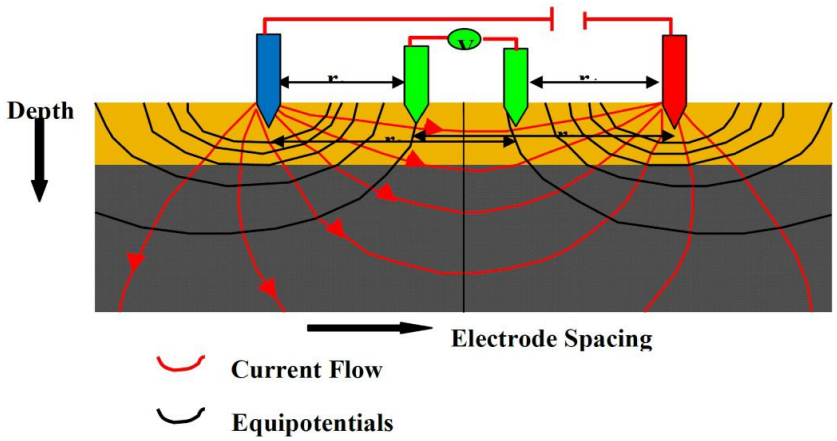

Figure 1: Basic Field Layout of DC Resistivity Survey (modified from Telford *et al*., 1990)

Figure 2: Abem Terrameter SAS 1000 used for the Data Acquisition showing the 4 Electrodes, the Cable Rollers and the Terrameter Box Device

Location of The Study Area

Molko is located in the Kwami Local Government Area of Gombe State. It lies at specific longitude and latitude coordinates in the northern part of Gombe, the capital of Gombe State, approximately 18 km along the Gombe-Ashaka road (Figure 4). It borders Medugu to the north, Zango Maguddu to the south, Yaiwa to the southeast, and Funakaye Local Government Area to the east, all within Gombe State.

The average altitude of Molko ranges from 360 to 400 meters above mean sea level (Figure 3)

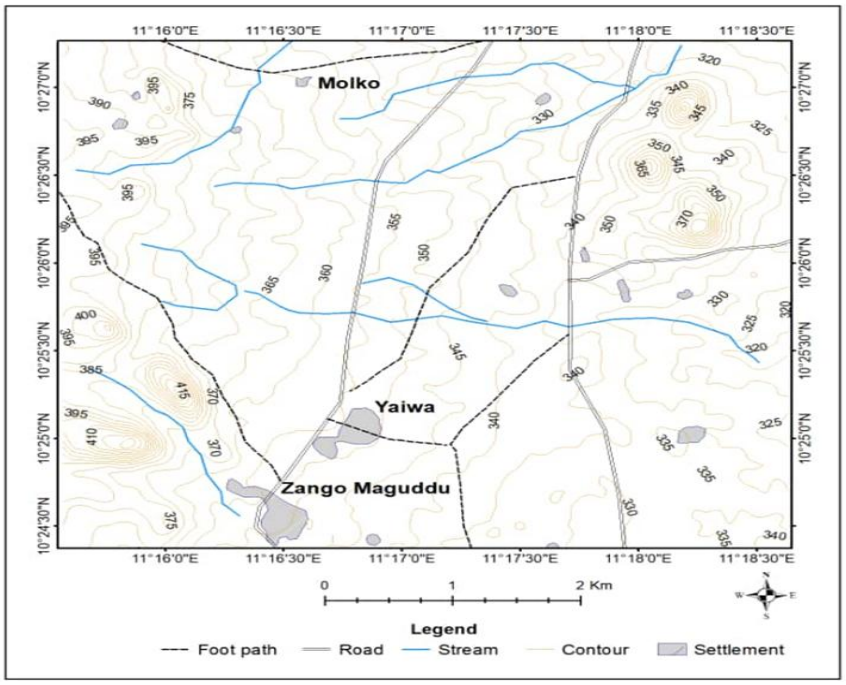

Figure 3: Topographical Map of Study Area and its Environs

Location, Climate and Vegetation of the Study Area

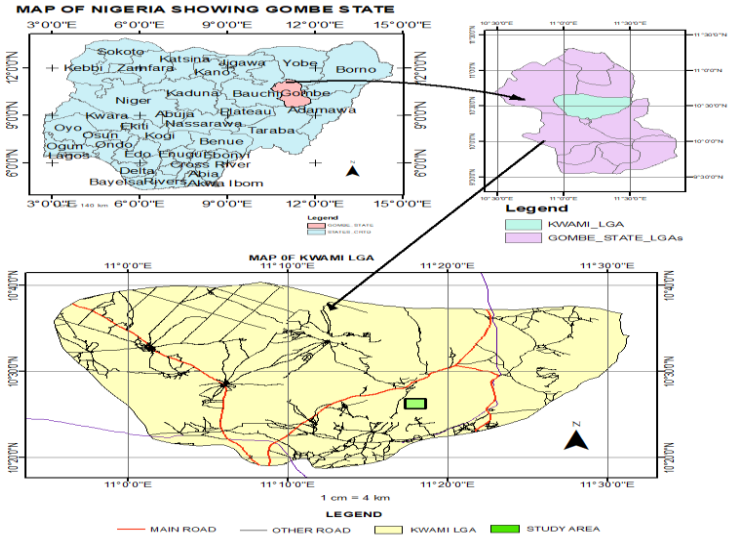

Figure 4: Map of Kwami LGA showing Study Area

Geology of the Study Area

The study area is located within a section of the Benue Trough, specifically in the Gongola Basin of the Upper Benue Trough, and lies within the Gombe Formation. The Gombe Formation hosts the coal seams in the Gongola Basin and lies conformably above the Yolde Formation. The Gombe Sandstone (Maastrichtian) contains sediments with coal-bearing seams (Obaje et al., 1998; Jauro et al., 2007). The study area is part of the Upper Benue Trough, geological structure underlying a large part of Nigeria and portion about Nigeria, extending Chad. It part of the broader West and Central African Rift System. The trough has its southern limit at the trough's where limit is is its down boundary, overlaid it recent downward and is overlain by northeasterly overlain by the Chad Basin, and is northeastward, Basin The trough is arbitrarily divided into lower, middle, and upper with the upper region further subdivided into the Gongola and Yola arms. The Anambra Basin in Basin, located west of western part lower region is region, is of the trough, being the a of compression, younger than the is considered it is having of during formation The formation. Trough was formed is still created part of the at The trough start first, the trough accumulated Initially, by basement and lakes. During the Late Early to Middle Initially, basin subsided rapidly sediments from covered by the sea.

Sea-inundated sediments accumulated, especially seafloor sediments under oxygen-deficient bottom conditions. In the Upper Cretaceous, the Benue Trough probably likely the main link connection the Gulf of likely served Guinea (the predecessor Sea) the the Chad and Iullemmeden Sea

connection) the end of this (the predecessor the basin rose above sea period, extensive coal forming Toward developed, particularly leading to the development of the Anambra coal-forming swamps, to contain 5,000 m leading region. The the development of Cretaceous contain approximately swamps, meters of sediment, contributing al., 2007) formation approximately meters coal deposits

The Yolde Formation lies conformably on the Bima Sandstone. In the Gongola Arm, the Pindiga Formation lies conformably on the Yolde Formation. Lithologically, this formation is characterized by dark/black carbonaceous shales and limestones, intercalated with pale-colored limestones, shales, and minor sandstones. The type locality of the Pindiga Formation is at Pindiga village. The Pindiga Formation is subdivided into three members, namely: Kanawa, Deba-Fulani, and Fika members in the Gombe Sub-basin (Zaborski, 1997). In the Gombe area of the Upper Benue Trough, poorly developed coalfields occur within the Gombe Sandstone, also of Maastrichtian age. The Gombe Sandstone, however, contains coal, lignite, and coaly shale intercalations, which in some places are very thick (Obaje, 2009). Fig. 2 shows the stratigraphic successions in the Upper Benue Trough (Gongola Arm).

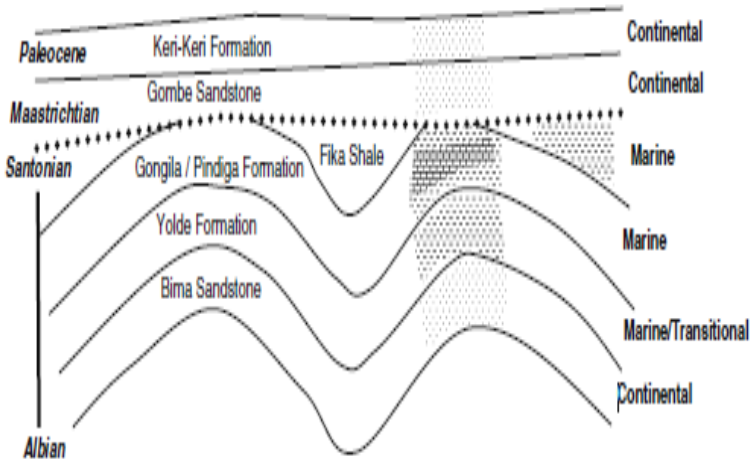

Figure 5: Stratigraphic Successions in the Upper Benue Trough (Gongola arm) (Obaje, 2009)

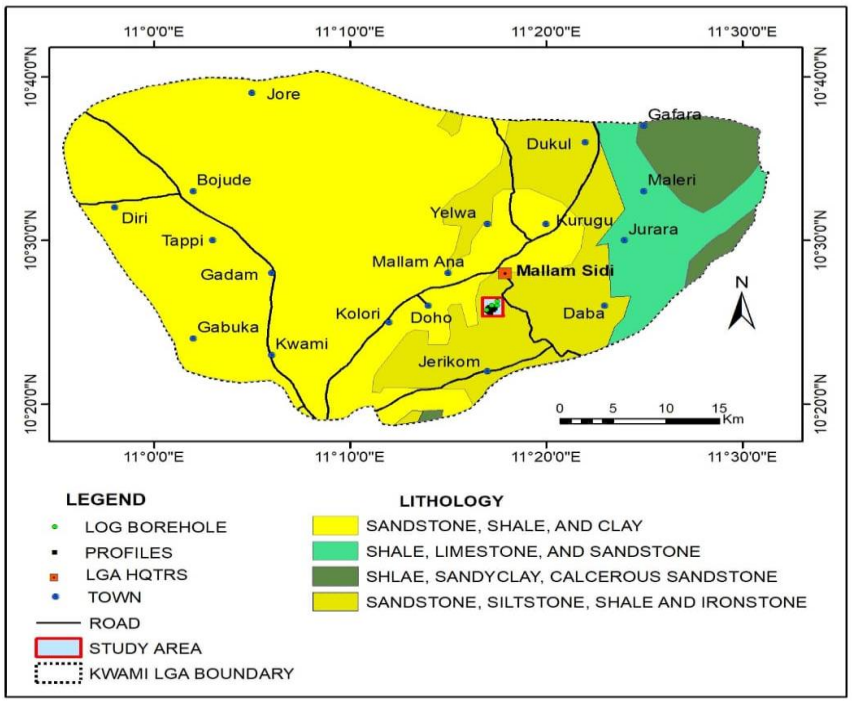

Figure 6: Geological Map of Kwami Local Government Area of Gombe State

Coal Formation

Coal is a sedimentary rock formed from the accumulation of altered dead plant remains, macerals, minerals, and water that became lithified at burial depth (Figure 7). Coal deposits are characteristic of thick, non-marine sedimentary basins that have dominated certain areas of the world at different times in the past (Van Krevelen, 1957; Francis, 1961; Gluskoter, 1975; Taylor et al., 1989; Speight, 2012; Speight, 2015).

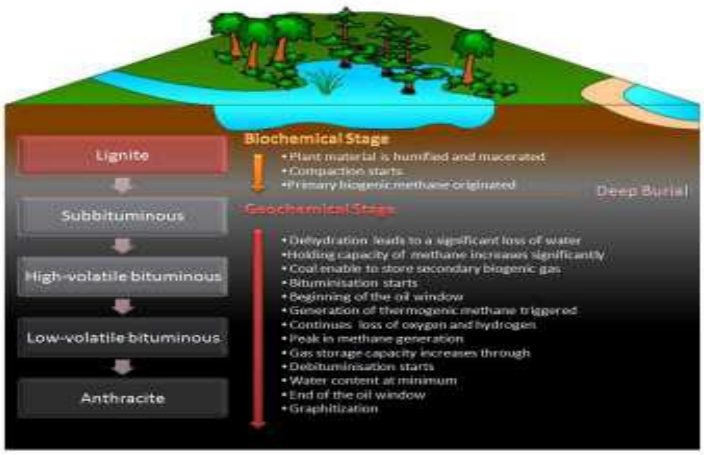

Figure 7: Coalification Stages During Coal Generation (Langenberg, *et al*., 1990)

The continuous transformation of plant material from peat to coal, known as coalification, can be divided into biochemical and geochemical stages. During the biochemical stage—biogenesis, which represents the early phase of coalification—low drainage rates and a lack of freshwater create an acidic, low-oxygen environment conducive to anaerobic microbial communities. These conditions minimize decomposition and promote the accumulation of carbonaceous material. As overlying inorganic sediments continue to deposit, this stage concludes at depths of several hundred meters, where percolating water that supplies microorganisms with nutrients is no longer available (Kim, 1978). The degree of maturation at this point is referred to as coal rank, with coal classified from lignite up to sub-bituminous (Langenberg et al., 1990).

Gradually, coalification progresses into the geochemical stage, during which the sediment undergoes diagenesis primarily driven by temperature (thermogenesis) and, to a lesser extent, pressure (Rightmire, 1984). With increasing depth, plant materials release volatile matter—including water, carbon dioxide, and light hydrocarbons—and become progressively enriched in carbon and structurally more homogeneous (Kim, 1978; Langenberg et al., 1990; Teichmüller and Teichmüller, 1968). At the culmination of the coalification process, coal reaches its highest rank, classified as meta-anthracite. Thus, the duration of heating and pressure at burial depth, carbon content, and the amount of heat energy produced classify coal into four main types or ranks: lignite, sub-bituminous, bituminous, and anthracite. Lignite (brown coal) is the lowest rank, containing 25–35% carbon and 45–60% moisture, resulting in the lowest energy content, ranging from 4,000 to 8,000 Btu per pound. Lignite is primarily burned in power plants to generate electricity.

Sub-bituminous coal is black in color and has a higher heating value than lignite, containing about 35-45% carbon. However, its moisture content lowers its heating value to between 8,000 and 13,000 Btu per pound. This coal is typically found very near the surface, which contributes to its lower energy values. Bituminous coal appears shiny and smooth and has distinct layers, as it forms when sub-bituminous coal undergoes increased levels of organic metamorphism (i.e., exposure to high heat and pressure). It contains 45-86% carbon and has two to three times the heating value of lignite. Bituminous coal is used to generate electricity and serves as an important fuel and raw material for the steel and iron industries. Anthracite is the highest grade of coal, with the highest heating value, containing between 86-98% carbon and a moisture content of 15-20%. When burned, it produces very little ash and pollutants other than carbon dioxide. Anthracite is hard and brittle, having experienced high temperatures and pressures during its formation, which explains why most of it is found deep within the earth (Kim, 1978). Coal formation is a dynamic process influenced by a wide variety of factors; therefore, there is no single molecular structure that represents a coal molecule. Its heterogeneity in structure and composition is too great. For simplicity, coal can be described as a structure formed by clusters of weakly linked aromatic rings that break down thermally during coalification, realigning and liberating volatiles (CO_2, CH_4, and H_2O) and hydrocarbons in a continuous process (Kim, 1977).

Coal is extracted from a deposit through several distinct steps, including prospecting, analysis of the mine's profit potential, mining, and final reclamation of the land after the mine is closed. Prospecting involves investigations using geological sciences, geophysical and geochemical methods, and drilling technologies to assess future demand. Among these, geophysical methods play a key role in coal seam mapping to estimate resources and evaluate economic potential before mining operations begin. This is followed by an analysis of the deposit to assess its financial viability, which informs the mining company whether to develop the mine. If approved, coal is mined in situ using equipment such as draglines, electric or hydraulic shovels, or bucket-wheel excavators. Two modern mining methods are typically employed: opencast (surface) mining and deep (underground) mining (Gluskoter, 1975; Vorres, 1993; Hartman, 2002; Ward, 2003). Raw coal is then processed in a preparation plant (e.g., oscillating column) to remove impurities such as rock, ash, and sulfur, thereby improving its value before utilization. The process involves crushing, screening into different sizes, and separation by physical and chemical methods to eliminate undesired impurities like water, ash, and sulfur, followed by briquetting for the intended use. Commercial uses of coal vary by type and include fuel feedstock for industrial processes such as electricity generation, steel production, cement manufacturing, and domestic consumption (see Figure 2.2). The properties that determine the economic viability and end-use category of coal are its rank (degree of coalification), chemical composition, and physical properties. Reason: The text was revised to improve clarity, flow, and technical accuracy. Grammar, punctuation, and spelling errors were corrected. Vocabulary was enhanced for precision and readability, and sentence structure was adjusted to ensure coherence and logical progression of ideas. Technical terms

were clarified, and redundant or awkward phrasing was eliminated.

MATERIALS AND METHODS

Reconnaissance Survey

Reconnaissance surveys were conducted to collect information about the study area. Initially, previous studies of the area and its surroundings were reviewed. Subsequently, the study area was visited to observe the terrain and identify potential locations suspected of containing coal deposits. GPS coordinates were recorded at strategic points to mark the locations where profiles would be established.

Choice of Array Configuration for the Survey

The dipole-dipole array configuration was employed for the field survey (Figure 8). This array is highly sensitive to resistivity variations beneath the electrodes in each dipole pair and is particularly responsive to horizontal variations with depth. Consequently, it is the most effective array for detecting three-dimensional structures among common arrays and exhibits low electromagnetic coupling between the current and potential circuits (Dahlin and Loke, 1997). Therefore, this array was selected for its sensitivity to 3D structures, its efficiency in areas with significant lateral variations in bedrock depth, and its excellent horizontal data coverage. As a result, it is well-suited for detecting coal deposits (Dahlin and Zhou, 2004).

In the electrode arrangement, the potential electrodes M and N are not positioned between the current electrodes A and B. The dipole-dipole array is generally the most convenient configuration used in the field, especially for large-scale surveys. In this type of array, all four electrodes are aligned along the same line, with the distance between the current electrodes A and B equal to the distance between the potential electrodes M and N, denoted by 'a'. The distance between the midpoints of the current and potential electrode pairs is an integer multiple of 'a', represented by the factor 'n'. .

The geometric factor K can be found from the following expression: $K = \pi n(n + 1)(n + 2)a$

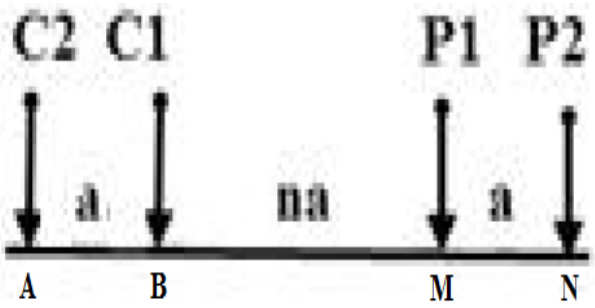

Figure 8: The Dipole-dipole Array Configuration (Zhou *et al.*, 2000)

Several factors can influence the results of an electrical resistivity survey, including porosity and saturation, mineral composition, electrolyte concentration, geological heterogeneity, electrode contact quality, instrument calibration, and cultural noise. Fluids such as water containing salts and chemicals conduct electricity, so higher water saturation decreases resistivity. Conversely, dry or poorly saturated materials exhibit higher resistivities. The mineral composition of subsurface materials significantly impacts resistivity measurements; for example, metals are good conductors, whereas certain rocks, like sandstone and coal, have higher resistivities. Geological heterogeneity, such as the presence of different rock layers or structures, can cause variations in resistivity. Therefore, understanding the geological setting is crucial for accurate interpretation of resistivity data. The quality of contact between electrodes and the ground is critical; poor contact can introduce errors and degrade data quality. Careful electrode placement and ensuring good contact are essential for obtaining reliable data. Proper calibration of resistivity measurement equipment is also important for accurate data interpretation. Electrical resistivity surveys can be affected by anthropogenic factors, such as nearby power lines, metal structures, or other sources of electrical interference, which may introduce noise into the data. We carefully considered all these factors during the acquisition and interpretation of the ERT data.

Common rocks	Resistivity (Ω-m)
Topsoil	50-100
Loose sand	500–5000
Gravel	100–600
Clay	1–100
Weathered bedrock	100–1000
Sandstone	200–8000
Limestone	500–10 000
Greenstone	500–200 000
Gabbro	100–500 000
Granite	200–100 000
Basalt	200–100 000
Graphitic schist	10–500
Slates	500–500 000
Quartzite	500–800 000
Ore minerals	
Pyrite (ores)	0.01–100
Pyrrhotite	0.001–0.01
Chalcopyrite	0.005–0.1
Galena	0.001–100
Sphalerite	1000–1 000 000
Magnetite	0.01–1000
Cassiterite	0.001–10 000
Hematite	0.01–1 000 000

Figure 9: Common Rocks and their Resistivity

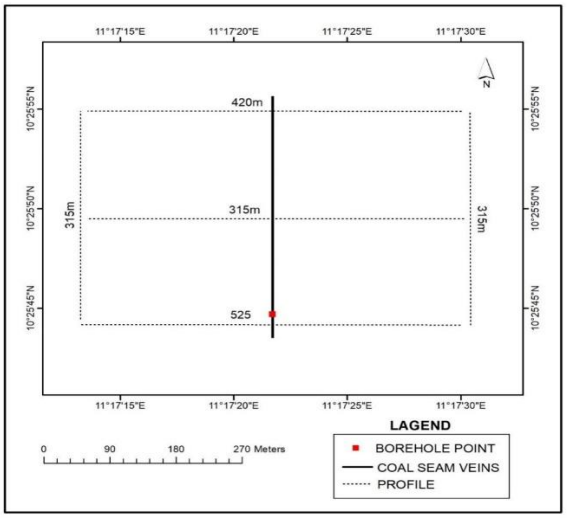

Figure 10: Google Earth Map of the Study Area showing the Profile Layout at the Study Area

The measurement of electrical resistivity imaging for Profile One was conducted at the borehole location to directly determine resistivity variations within the coal-bearing layers. These resistivity values served as a reference for interpreting coal layers in the other profiles

Correlation of Borehole log Data with Pseudo-Section of 2D Electrical Resistivity Imaging

Geologic Section from Borehole Data

Borehole log are often use to correlate results obtained as from geophysical method as this survey method is direct. This often done by correlating the resistivity values obtained from ths study area with lithological information obtained from the study area. Boreholes log are reliable sources of primary data provide and electrical resistivity imaging interpretation provide secondary information. Although borehole data provide a good subsurface sample for a six-inch diameter vertical cylindrical volume, it can be poor representation of the several sequare meters surrounding the borehole

meters			Lithology	Lithological description
Depth from	Depth To	thickness		
0.00	25.00	25.00		Overburden
25.00	28.70	3.70		Coal
28.12	28.66	0.54		shaly SANDTONE
28.66	30.90	2.24		Coal
30.26	33.00	2.74		SHALE
33.00	36.00	3.00		SANDTONE
36.00	36.11	0.11		Coal
36.73	37.05	0.32		shale
37.05	37.18	0.13		shaly Coal
37.18	38.06	0.88		shale
38.06	40.76	2.70		SANDTONE
40.76	50.00	9.24		

Figure 11: Electrical Resistivity Imaging

The borehole is located at latitude 1,154,272 N and longitude 1,154,272 E. It was drilled to a depth of 48 meters. The overburden was encountered from 0.00 m to 25.00 m, with a thickness of 25 m. A coal seam was found between 25.00 m and 28.66 m, measuring 3.70 m thick, followed by shaly sandstone from 28.12 m to 28.66 m, with a thickness of 0.54 m. Another coal seam was observed from 28.66 m to 30.50 m, with a thickness of 2.24 m, followed by shale from 30.26 m to 33.00 m, measuring 2.74 m thick. Sandstone was encountered from 33.00 m to 36.00 m, with a thickness of 3 m. The third coal seam was observed from 36.00 m to 36.11 m, with a thickness of 0.11 m, followed by shale from 37.10

m to 37.30 m, measuring 0.20 m thick. Shaly coal was discovered from 37.18 m to 38.00 m, with a thickness of 0.82 m. Shale was found from 38.00 m to 40.70 m, with a thickness of 2.70 m. Finally, sandstone was observed from 40.70 m to 48.00 m, with a thickness of 7.30 m.

Correlation of 2d Resistivity Section with Borehole Log

The 2D electrical resistivity imaging revealed variations in subsurface materials at different depths along each transverse profile, as well as their resistivity values at various layers. The borehole log indicated the depth range of subsurface materials from 0.00 m to 38.00 m, with the following stratigraphy: 0.00 m to 2.00 m (2.00 m thickness) overburden; 25.00 m to 28.70 m (3.70 m thickness) coal; 28.12 m to 28.16 m (0.54 m thickness) shaly sandstone; 28.66 m to 30.90 m (2.24 m thickness) coal; 30.26 m to 33.00 m (2.74 m thickness) shale; 33.00 m to 36.00 m (3.00 m thickness) sandstone; 36.00 m to 36.11 m (0.11 m thickness) coal; 36.11 m to 37.05 m (0.94 m thickness) shale; 37.18 m to 38.00 m (0.82 m thickness) shale; and 37.18 m to 38.00 m (0.88 m thickness) shaly coal. This depth range corresponds well with the 2D electrical resistivity imaging of profile one, which shows low resistivity values ranging from 1 Ω·m to 100 Ω·m, representing overburden; relatively high resistivity values between 400 Ω·m and 1000 Ω·m, indicating coal seams; and high resistivity zones from 1500 Ω·m to 5000 Ω·m, corresponding to sandstone, shale, and carbonaceous zones. This correlation demonstrates the consistency between the borehole log and the 2D electrical resistivity inversion across the five established profiles. Furthermore, the 2D electrical resistivity imaging revealed the lateral extent of lithological formations in the subsurface, which the borehole log alone could not capture. This clearly highlights the importance of integrating electrical resistivity imaging into various subsurface investigations. Reason: The original text contained numerous grammatical errors, inconsistent units and measurements, unclear phrasing, and lacked proper punctuation. The revision improves clarity, technical accuracy, and readability by restructuring sentences, correcting measurements, standardizing terminology, and enhancing vocabulary while preserving the original meaning. During data processing, a series of steps were taken to remove spurious noise and irrelevant signals from the collected data to ensure accurate interpretation of the relevant signals. The measured apparent resistivity data files for all resistivity imaging profiles were downloaded from the ABEM ES464 Terrameter onto a computer using a rewritable compact disc. The computer had the ABEM file conversion software (SAS4000 Utilities) and the RES2DINV application installed. The SAS4000 Utilities software was used to convert the original data files (in .s4k format) into the appropriate .DAT format input files readable by the inversion software (RES2DINV). A total of nine files were converted for processing using RES2DINV (Loke & Barker, 1996). However, these resistivity data sets were first inspected for the presence of unreasonably high or low (negative) resistivity values, referred to as "bad data points" (Loke, 2010). If any such points were found, they were manually removed by simply clicking on them, as illustrated in the figure, before compiling the resistivity model or ERI resistivity profile that displays horizontal and vertical resistivity distribution.

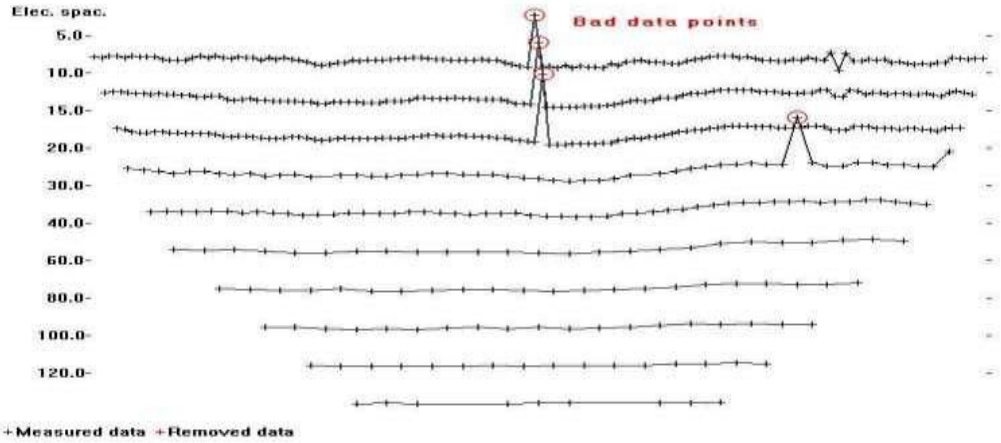

Figure 12: An Example of a Profile Showing Data Set with a few Bad Data Points (Loke, 2010)

The RES2DINV software is a computer program that automatically generates a 2D resistivity model and an IP model of the subsurface from an electrical survey using an inversion routine that divides the subsurface into rectangular blocks (Loke & Barker, 1996). Two inversion techniques are commonly used in resistivity data inversion: the standard least-squares smoothness constraints and the robust constraint inversion techniques (see Figure 3.5). The standard constraint inversion technique, also called the L2 norm, was used. This method is based on the following equation:

$(JTJ + \lambda F)\Delta QK = JTg - \lambda FQK$ (3.2)

where

$F = \alpha x Cx$

$T Cx + \alpha z Cz$

$T Cz$

Cx = Horizontal roughness filter

Cz = Vertical roughness filter

J = Jacobian matrix of partial derivatives

JT = Transpose of J

λ = Damping factor

Q = Model change vector

g = Data misfit vector

C x

T= Transpose of horizontal roughness filter

C z

T= Transpose of vertical roughness filter

In this technique, the least-squares method minimizes the square of the differences between the observed and calculated apparent resistivity values. Simultaneously, it also attempts to minimize the squares of the changes in the model resistivity values (deGroot-Hedlin & Constable, 1990). This approach produces a subsurface model with smoothly varying resistivity values. Such a model is appropriate in environments where subsurface resistivity changes gradually

(Loke et al., 1999). This method yields reasonable results only if the data contain random, or "Gaussian," noise. However, if the dataset includes "outlier" data points—noise originating from non-random sources such as errors or equipment malfunctions the results will be less reliable. This is because such outliers can have a significant impact.

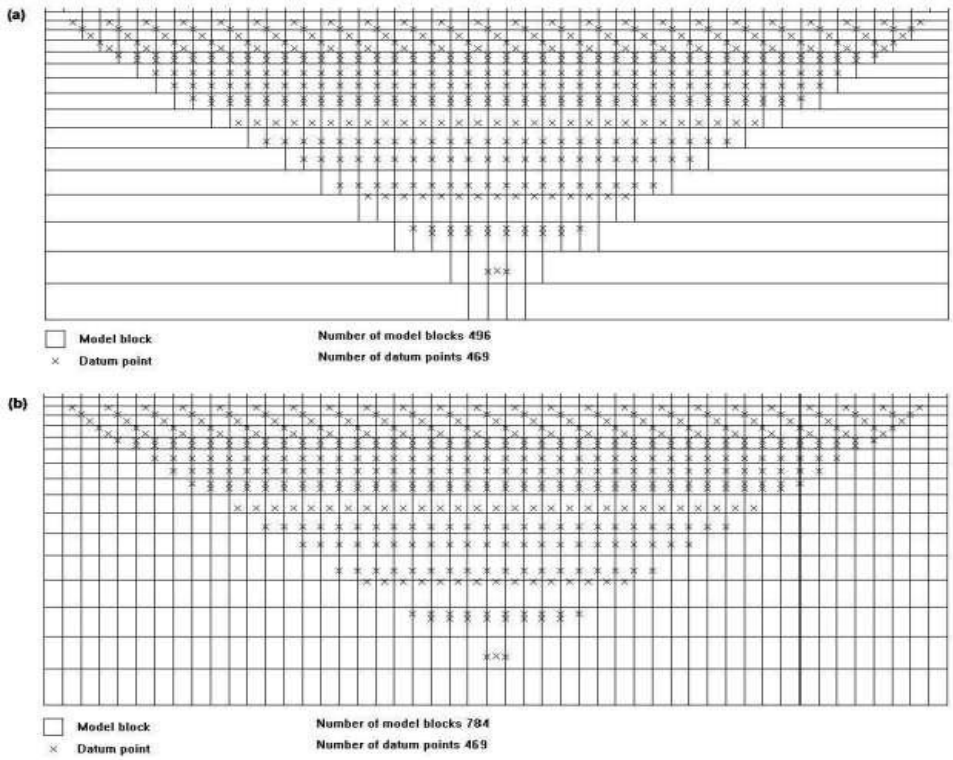

Figure 13: (a), (b) are Two Possible Arrangements of the Blocks used in a 2-D Model Together with the Datum Points in the Pseudo Section (Edwards, 1977)

The program calculates apparent resistivity values using the finite-difference method and iteratively compares them to the measured data to minimize the difference. During iteration, the modeled resistivity values are adjusted until the calculated apparent resistivity values align with the actual measurements. The iteration process stops only when the inversion converges, as indicated by the root-mean-squared (RMS) error either when the RMS error falls below an acceptable threshold, typically less than 5%, or when the change in RMS error between consecutive iterations becomes negligible. However, the model with the lowest possible RMS error can sometimes exhibit unrealistically large resistivity values, and therefore may not always represent the best geological model. Consequently, the most prudent approach is to select the model at the iteration where the RMS error stabilizes, usually between the 3rd and 5th iterations. A model is accepted at the iteration beyond which the RMS error no longer changes significantly, typically between the 8th and 10th iterations. The final output displayed after inversion includes the measured and calculated apparent resistivity pseudo-sections, as well as the inverse model showing true depth and true formation resistivity.

RESULTS AND DISCUSSION

The electrical resistivity imaging for Profile One was conducted at the borehole location to directly assess resistivity variations within the coal-bearing layers. These resistivity values served as a reference for interpreting coal layers in the other profiles. The borehole log data correlated with the 2D electrical resistivity pseudo-section, allowing determination of resistivity values, depth, and thickness of the subsurface materials. A low resistivity range of 1.33 Ωm to 16.3 Ωm corresponds to the overburden, as indicated by the borehole log data. A relatively high resistivity zone, ranging from 478 Ωm to 1000 Ωm, corresponds to the coal seams when integrated with the borehole data. This zone extends laterally from approximately 98 m to 350 m, from the western to the eastern part of the study area, at a depth of 20 m to 25 m, with a thickness of about 5 m. Additionally, a high resistivity zone ranging from 1550 Ωm to 5031 Ωm consists of shaly sandstone.

2D ERT Inversion Result

Profile One

The 2D inversion of electrical resistivity imaging revealed that Profile One consists of three distinct layers, with resistivity values ranging from 1.33 Ωm to 5031 Ωm at depths of up to approximately 39 meters below the surface. The top layer exhibits resistivity values between 1.33 Ωm and 300 Ωm. The low resistivity values, ranging from 1.33 Ωm to 16.3 Ωm, correspond to overburden and wet clay. The second layer has resistivity values between 400 Ωm and 1400 Ωm, while the third layer ranges from 1550 Ωm to 5031 Ωm and likely consists of carbonaceous black shale to silty shale. The second layer is probably the host of the coal seams, with relatively high resistivity values ranging from 478 Ωm to 1000 Ωm. These resistivity values for the coal seam were determined based on the correlation between the 2D inversion of electrical resistivity imaging and borehole logs.

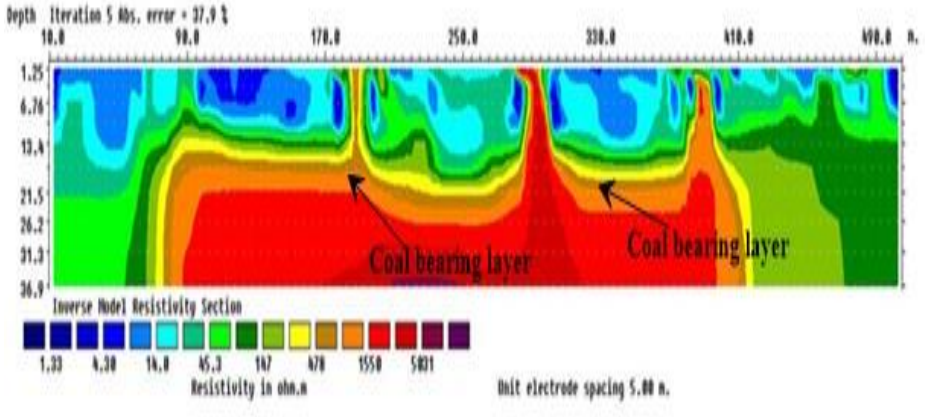

Figure 14: Inverse Resistivity Model of Profile One

Profile Two

The 2D inversion of electrical resistivity imaging revealed that Profile two consists of three distinct layers, with resistivity values ranging from 7.81 Ω·m to 193,886 Ω·m at depths of up to approximately 36 meters below the surface. The top layer exhibits resistivity values between 7.81 Ω·m and 400 Ω·m. The low resistivity values, from 7.81 Ω·m to 72.1 Ω·m, indicate the presence of wet clay. The second layer has resistivity values ranging from 400 Ω·m to 1,400 Ω·m, while the third layer ranges from 1,550 Ω·m to 193,886 Ω·m and likely consists of carbonaceous black shale to silty shale. The second layer is likely the host of the coal seams, with resistivity values between 400 Ω·m and 1,000 Ω·m.

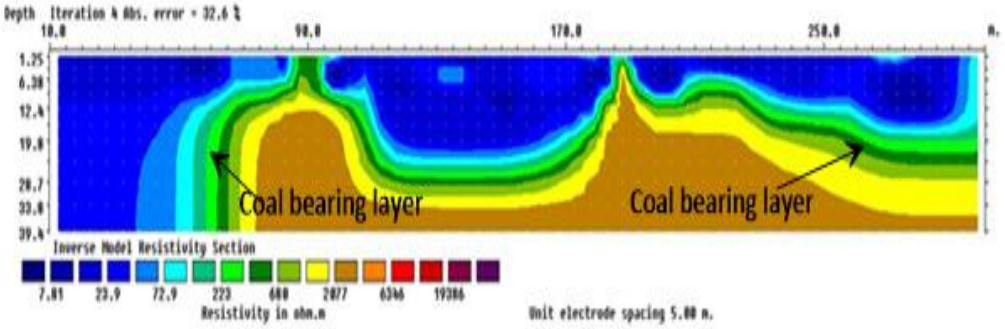

Figure 15: Inverse Resistivity Model of Profile Two

Profile Three

The 2D inversion of electrical resistivity imaging revealed that Profile three consists of three distinct layers, with resistivity values ranging from 2.11 Ωm to 236,880 Ωm at depths of up to approximately 39 meters from the surface. The top layer exhibits resistivity values between 7.81 Ωm and 400 Ωm. The low resistivity values, from 7.81 Ωm to 52 Ωm, indicate the presence of wet clay. The second layer has resistivity values ranging from 400 Ωm to 1,400 Ωm, while the third layer ranges from 1,550 Ωm to 193,886 Ωm and likely consists of carbonaceous black shale to silty shale. The second layer is likely the host of the coal seams, with resistivity values between 400 Ωm and 1,000 Ωm. These resistivity values for the coal seam were determined based on the correlation with the 2D inversion of electrical resistivity imaging of Profile One.

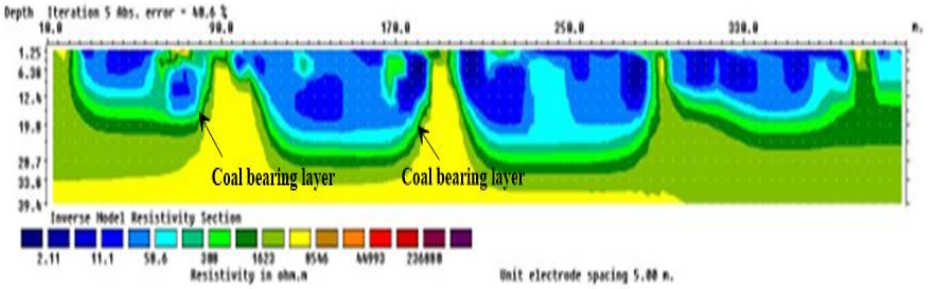

Figure 16: Inverse Resistivity Model of Profile Three

Profile Four

The 2D inversion of electrical resistivity imaging revealed that Profile four consists of three distinct layers, with resistivity values ranging from 1.27 Ωm to 1473 Ωm at depths of up to approximately 39 meters from the surface. The top layer exhibits resistivity values ranging from 7.81 Ωm to 400 Ωm. The low resistivity values, from 1.27 Ωm to 72.1 Ωm, indicate the presence of wet clay. The second layer has resistivity values between 400 Ωm and 1400 Ωm, while the third layer ranges from 1400 Ωm to 1473 Ωm and likely consists of carbonaceous black shale to silty shale. The second layer is likely the host of the coal seams, with resistivity values ranging from 400 Ωm to 1000 Ωm. These resistivity values for the coal seam were determined based on the correlation with the 2D inversion of electrical resistivity imaging of Profile One.

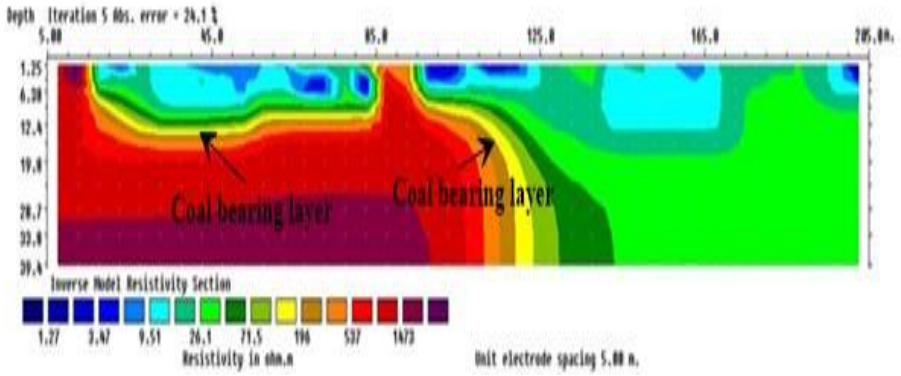

Figure 17: Inverse Resistivity Model of Profile Four

Profile Five

The 2D inversion of electrical resistivity imaging revealed that Profile five consists of three distinct layers, with resistivity values ranging from 7.34 Ω·m to 44,619 Ω·m at depths of up to approximately 39 meters from the surface. The top layer exhibits resistivity values ranging from 1.86 Ω·m to 400 Ω·m. The low resistivity values, from 1.27 Ω·m to 79 Ω·m, indicate the presence of wet clay. The second layer has resistivity values between 400 Ω·m and 1,400 Ω·m, while the third layer ranges from 1,400 Ω·m to 1,473 Ω·m, likely composed of carbonaceous black shale to silty shale. The second layer is likely the host of the coal seams, with resistivity values ranging from 400 Ω·m to 1,000 Ω·m. These resistivity values for the coal seam were determined based on the correlation with the 2D inversion of electrical resistivity imaging of Profile One.

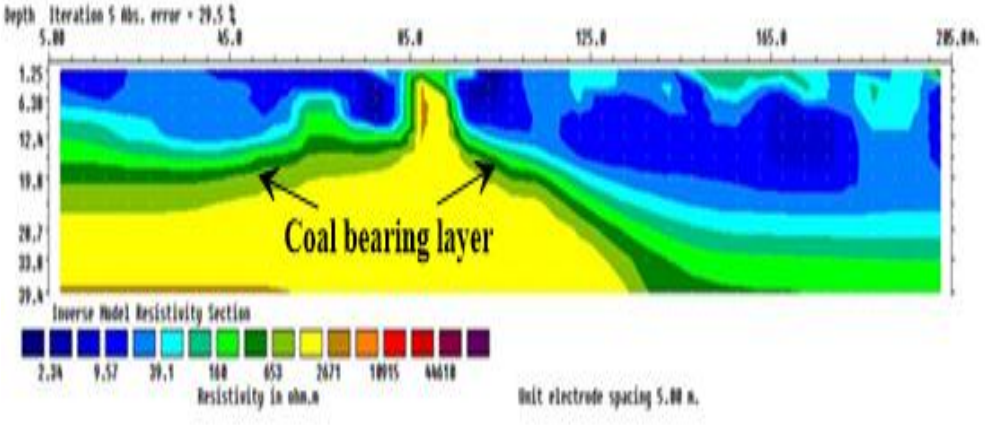

Figure 18: Inverse Resistivity Model of Profile Five

Correlation of Profiles for the Detection of Continuity of the Subsurface Structures

The resistivity model for each profile was aligned according to the map illustrating the layout of the profiles, with the aim of ascertaining the continuity of subsurface structures and, by inference, detecting the trend of the coal deposit. Coal occurs in strata, applying Steno's Principle of Lateral Continuity, which states that "material forming any stratum was continuous over the surface of the Earth unless some other solid bodies stood in the way" (Stovall, 1955). Where lateral continuity of the strata is absent, erosion or faulting can be inferred. This principle is applicable to the correlation of strata. The resistivity models of the merged profiles are shown in Figure 15 below.

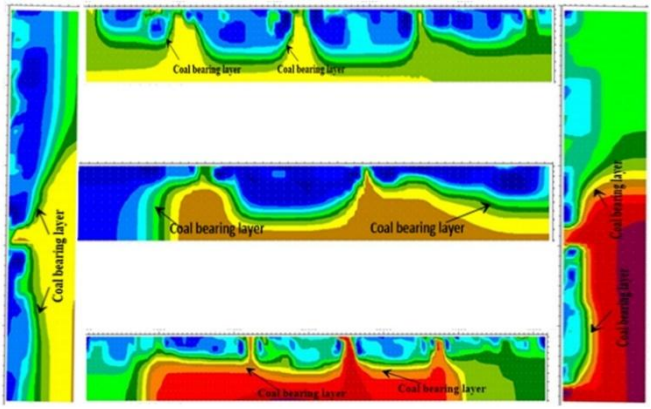

Figure 19: 2D Resistivity Fence Diagram of Five Profiles showing Resistivity Distribution

Mohammed et al., (2017) al. 2D electrical resistivity imaging utilizing Wenner-Schlumberger using the to delineate the strike direction of coal in Tai in the area of Gombe, northeastern Nigeria, inter Nigeria. They used an inter-electrode 2 m, the m to generate electrical resistivity pseudo section pseudosection model revealed a depth of 17 meters from the surface, with resistivity values ranging from 361 Ω m to 843 Ω m. This was interpreted as coal occurring at depths between 7 meters and 17 meters, with a thickness of 10 meters. The study area is located approximately 75 km from Molko Village.

Table 1: Correlation between Study Areas; Molko and Tai vallage

Study area	Molko village	Tai village
Resistivty values range of a coal	400 ωm to 1000 ωm	361 ωm to 843 ωm
Depth of the coal seam	21 m to 26 m	7 m to 17 m
Thickness of the coal seam	2 m to 4 m	7 m 10 m
depth penetration from the surface	39 m	17 m

*i. **Greater Depth of Investigation***

A 5 m spacing allows for a significantly deeper investigation depth compared to 2 m, which is essential for identifying deeper coal seams or mapping voids/subsurface features that lie beneath shallow, highly conductive overburden (e.g., shale).

*ii. **Wider Coverage and Efficiency***

Using 5 m spacing results in a longer survey line per set of electrodes, providing a broader overview of the coal field's structural features, such as major faults or larger areas of coal seam continuity.

*iii. **Optimal Compromise for Regional Mapping***

While 2 m spacing provides higher shallow resolution, 5m spacing is often considered the ideal, cost-effective compromise for identifying lateral continuity and thickness of coal seams at moderate depths (e.g., 10–25 meters), which is typical in many regional coal studies.

CONCLUSION

Electrical resistivity imaging surveys were successfully conducted in Molko Village, Gongola Basin, Kwami Local Government Area of Gombe State, Northeastern Nigeria, using a dipole-dipole electrode configuration to visualize subsurface resistivity for the investigation of coal deposits. Measurements were carried out along five profiles. The Res2DInv software was employed for data processing. The 2D inversion results of the electrical resistivity imaging correlated well with borehole data. The findings reveal resistivity variations of the suspected coal seam across different profiles. The five established profiles showed coal resistivity values ranging from 400 Ω·m to 1000 Ω·m at depths of approximately 20 to 25 meters, with thicknesses ranging from 2 to 4 meters. The resistivity variations observed in this study align well with findings from previous research on coal resistivity, with sandstone serving as the host rock in the study area, and demonstrate significant potential for mining. Based on the results of this research, it is recommended that further investigations using 3D electrical resistivity and seismic refraction methods be conducted to complement and confirm the findings obtained from 2D electrical resistivity surveys.

REFERENCES

Aberšek, B.; Flogie, A. Energies and Energetics. In Human Awareness, Energy and Environmental Attitudes; Springer International Publishing: Cham, Switzerland, 2022; pp. 91–110.

Adli, Z. H., Musa, M. H., & Arifin, M. N. K. (2010). Electrical Resistivity of Subsurface: Field and Laboratory Assessment, 4(9), 799–802.

Anderson, N. L., Croxton, N., Hoover, R., & Sirles, P. (2008). Geophysical methods commonly employed for geotechnical site characterization. Transportation Research Circular(E-C130).

Arjwech, R., Everett, M., Briaud, J. L., Hurlebaus, S., Medina, C. Z., Tucker, S., &Yousef pour, N. (2013). Electrical resistivity imaging of unknown bridge foundations. *Near Surface Geophysics, 11*(6), 591-598.

Arjwech, R., and Everett, M. E. (2015). Application of 2D electrical resistivity tomography to engineering projects: Three case studies. *Songklanakarin Journal of Science &Technology, 37*(6), 675 – 681.

Dahlin, T. (2001). The development of DC resistivity imaging techniques. *Computers &Geosciences*, *27*(9), 1019-1029

Dahlin, T., & Zhou, B. (2004). A numerical comparison of 2D resistivity imaging with 10 electrode arrays. *Geophysical prospecting*, *52*(5), 379-398.

Dahlin, T., & Loke, M. H. (1997). Quasi-3D resistivity imaging-mapping of three-dimensional structures using two-dimensional DC resistivity techniques. 3rd EEGS Meeting (pp. cp-95). European Association of Geoscientists & Engineers.

deGroot-Hedlin, C., & Constable, S. C. (1990). Occam's inversion to generate smooth, two-dimensional models from magnetotelluric data. *Geophysics*, *55*(12), 1613-1624.

Edwards, L.S., (1977), A modified pseudosection for resistivity and induced polarization. Geophysics, 42, 1020-1036.

Francis, W. (1961). *Coal: its formation and composition*. E. Arnold.

Gluskoter, H. J. (1975). Mineral matter and trace elements in coal.

Hartman, H. L., & Mutmansky, J. M. (2002). *Introductory mining engineering*. John Wiley & Sons.

Hatcher, P.G.; Clifford, D.J. The organic geochemistry of coal: From plant materials to coal. Org. Geochem. 1997, 27, 251–274. [CrossRef]

Hatherly, P. (2013). Overview on the application of geophysics in coal mining. International Journal of Coal Geology, 114, 74-84. doi: https://doi.org/10.1016/j.coal.2013.02.006

Kearey, P., Brooks, M., & Hill, I. (2002). *An introduction to geophysical exploration* (Vol. 4). John Wiley & Sons.

Kim, A. G. (1977). *Laboratory studies on spontaneous heating of coal: A summary of information in the literature* (Vol. 8756). Department of the Interior, Bureau of Mines.

Kim, A. G. (1978). *Experimental studies on the origin and accumulation of coalbed gas* (Vol. 8317). Department of the Interior, Bureau of Mines.

Langenberg, C.W., Kalkreuth, W., Levine, J.R., Strobl, R., Demchunk, T., Hoffman, G., Jerzykiewicz, T., (1990). Coal geology and its application to coal-bed methane reservoirs: lecture notes for short course, Edmonton, August 20-24, 1990. Alberta Research Council.

Lei, Y. (2015). Application of geophysical technique in the coal mining. *International Journal of Online Engineering* (iJOE), 11 (7), 11-13.

Loke, M. H., & Barker, R. D. (1996). Rapid least squares inversion of apparent resistivity Pseudo-sections by a quasi-Newton method 1. *Geophysical prospecting*, *44*(1), 131-152.

Loke, M. H., and Barker, R. D. (1996). Rapid least squares inversion of apparent resistivity pseudo-sections by a quasi-Newton method 1. *Geophysical prospecting*, *44*(1), 131-152.

Loke, M. H. (1999). Electrical imaging surveys for environmental and engineering studies. A practical guide to, 2.

Loke, M. H. (2010). RES2DINV ver. 3.59 for Windows XP/Vista/7. Rapid 2-D Resistivity & IP inversion using the least-squares method. *Geoelectrical Imaging 2D & 3D Manual. (Geotomo Software: Penang) Available at: www. geoelectrical. Com (verified June 2011)*.

Miller, B.G. Coal Energy Systems; Academic Press: Cambridge, MA, USA, 2005.

Mohammed M. A., Adewumi T., Ahmed A. L., & Lawal K. M. (2016). Electrical Resistivity Imaging of a Coal Deposit at Tai Area of Gombe State, North Eastern Nigeria. *Journal of Environment and Earth Science*. ISSN 2225-0948 (Online) Vol.6, No.6, 2016.

Obaje, N. G. (2009). Geology and Mineral Resources of Nigeria, Lecture Notes in Earth Sciences Springer-Verlag Berlin Heidelberg, pp. 57-68.

Rightmire, C.T., (1984). Coalbed Methane Resources of the United States. AAPG Special Volumes 138, 1–13.

Speight, J. G. (2012). *The chemistry and technology of coal.* CRC press.

Speight, J. G. (2015). *Handbook of coal analysis.* John Wiley & Sons.

Stovall, J. W. & Brown, H. E. (1955). *The Principles of historical* geology. Ginn.

Taylor, G. H., Liu, S. Y., & Diessel, C. F. K. (1989). The cold-climate origin of inertiniterich Gondwana coals. *International Journal of Coal Geology*, *11*(1), 1-22.

Thomas, L. (2012). Coal Geology. Chichester, UK: John Wiley & Sons, Ltd. https://doi.org/10.1002/9781118385685

Tiwary, S. N. (1993). Measurement of electrical resistivity of coal samples. Fuel, 72(8),1099-1102.

Teichmüller, M., Teichmüller, R., (1968). Geological Aspects of Coal Metamorphism, D. Murchison and T.S. Westoll. ed. Elsevier Publishing Co., New York.

Van Krevelen, D. W. (1957). Coal Science, Aspects of Coal Constitution.

Vorres K. S. (1993). *Users handbook for the Argonne premium coal sample program* (No. ANL/PCSP-93/1). Argonne National Lab., IL (United States)

Ward C. R. (2003). Coal exploration and mining geology. School of Geology, University of New South Wales, Sydney, Australia. *Geology*, V: 1 – 9.